

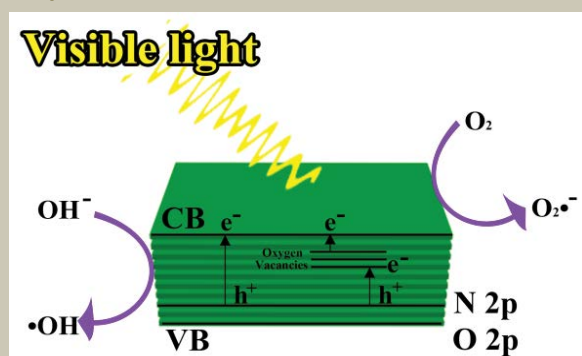
Enhanced Photocatalytic Response of N Doped Niobium Titanates Prepared by Ion Exchange Process

Mingming Zou¹, Lu Feng¹,
Erum Pervaiz^{1,2},
Ayyakannu Sundaram
Ganeshraja¹, Chuanxi Wang³
and Minghui Yang¹

Abstract

Herein we report the homogeneous and effective substitution of O by N in the layered titanates. The resultant materials HTiNbO_{5-x}N_x (350°C, 30 min) unveiled extraordinary band-to-band excitation and increased absorption intensity (induced by oxygen vacancies). Upward shift of valence band maximum by N 2p states is confirmed by photoelectron spectroscopy and is concluded as the source of band-to-band visible light excitation. The electrons generated upon visible light excitation in the conduction band of HTiNbO_{5-x}N_x (350°C, 30 min) had strong reduction ability, reducing O₂ into active O₂^{•-} radicals during photocatalysis. These findings are the clear evidence for the substantial role of doped N in achieving band-to-band visible-light photon excitation in layered titanates. The new physical insights into substitutional N in layered titanates with hydrogen bond (weak bond energy) gained here may have important implications for developing other efficient visible light photocatalysts by nonmetal doping.

Graphical Abstract:



Keywords: Substitutional N; Band-to-band excitation; Oxygen vacancies; Active O₂^{•-} radicals

- 1 Dalian Institute of Chemical Physics, Chinese Academy of Sciences, Dalian, 116023, China
- 2 School of Chemical and Materials Engineering (SCME), National University of Sciences and Technology (NUST), Islamabad, 44000, Pakistan
- 3 Ningbo Institute of Industrial Technology, Chinese Academy of Sciences, Ningbo, 315201, China

Corresponding author:
Minghui Yang

✉ myang@dicp.ac.cn

Dalian Institute of Chemical Physics, Chinese Academy of Sciences, 457 Zhongshan Road, Dalian, 116023, China.

Tel: 0411-84379600

Citation: Zou M, Feng Lu, Pervaiz E, et al. Enhanced Photocatalytic Response of N Doped Niobium Titanates Prepared by Ion Exchange Process. *Synth Catal.* 2016, 1:1.

Received: November 05, 2016; **Accepted:** December 02, 2016; **Published:** December 05, 2016

Introduction

Waste water treatment being the active focus for ongoing research areas, have emerged several techniques to cope with the problem. As one of the most attracted field, photocatalysis fascinated a range of scientific and technological interest for using in water purification and splitting fields. It provides easy and reckless removal of water contaminations using only solar energy in the presence of an active material. A lot of work being done on

these active materials to manipulate the band gaps, so that the material can be effectively utilized in the presence of sunlight, an abundant energy source. Most of the time, TiO₂ is considered as active material for photocatalysis owing to certain features and desirable properties (environmental friendly, facile synthesis, and high chemical stability), many research have focused on different structures of TiO₂ [1-2]. However, actual applications are restricted due to: (i) The relatively large band gap of anatase TiO₂ (around 3.2 eV) only requires UV light; (ii) Low separate rate of the

photoproducted electron-hole pairs [3]. Hence, many scientists took certain modifications in TiO_2 structures, for example doped with various transition-metal cations, nonmetals and coupled with a sensitizing dye or short band-gap semiconductor for improving the visible light performance [4-6]. In addition, many new visible light driven photocatalysts have been exploited.

Besides typical and modified semiconductor metal oxides, layered titanates (KTiNbO_5) have now been considered as new type of photocatalysts [7-9]. These inorganic layered compounds possess unique properties due to electrostatic interactions between laminates and interlayer ions that are comparable with TiO_2 (anatase) crystals in few respects. Firstly, special interlayer galleries amongst sheets which contained TiO_6 octahedra structure (with four edges) [10], secondly they have the ability of ion-exchange by H^+ ions and obtained original layered structure of interlayers titanium niobate (for HTiNbO_5). And the third important characteristic is, an excellent pathway facilitated the nitriding treatment which happens due to the layered galleries and weak binding energy of hydrogen bond [11]. However, HTiNbO_5 usually a wide bandgap semiconductor photocatalyst and can only be activated under UV light. UV light accounts for 5% of the solar energy spectrum as compared to visible light that occupies 46% of the whole electromagnetic spectrum [12], it is of great worth to synthesize a visible light-responsive HTiNbO_5 photocatalyst.

Generally, N-doping not only results into intermediary energy levels in the bandgap as consequences of either mingling N 2p with O 2p states or by introduction of localized states [13], but can also act as trapping centers for photogenerated charge carriers thereby effectively reduce their recombination [14-15]. The oxygen vacancies produced in the process of nitriding under ammonia gas would promote the absorption of visible light to a large extent. In the present work, subsequent calcination-ion-exchange-nitrogen doping method has been used to synthesize layered N doped titanioniobate with 6.15 atom % N content successfully. The samples were carefully characterized and enhanced performance was observed in photocatalytic degradation of Rhodamine B under visible light irradiation. Further, brief analysis of active radicals in terms of their oxidative potentials has also been discussed.

Experimental Method

Materials

All chemicals were analytical reagents and used without further purification. The anatase TiO_2 (99%, aladdin), Niobium (V) oxide (Nb_2O_5 , Sinopharm, China), Potassium carbonate (99%, K_2CO_3 , Sinopharm, China), absolute ethanol and deionized water were supplied by the Sigma-Aldrich, China. Nitric acid, Rhodamine B (AR grade, Sinopharm, China) was used as model organic pollutants for assessing the activity of synthesized materials. In all experiments, doubly distilled water was used.

Synthesis of layered KTiNbO_5 and protonated form HTiNbO_5

Layered KTiNbO_5 was synthesized by thermally treating a mixture

of K_2CO_3 , TiO_2 and Nb_2O_5 in a stoichiometric molar ratio of 1: 2: 1 at 650°C for 1 h and then at 1200°C for 24 h. The protonated form (HTiNbO_5) was obtained by curing the KTiNbO_5 with 5 M HNO_3 aqueous solution at room temperature for 3 days. During the proton exchange reaction, the acidic solution was replaced with a fresh one every 24 h.

Synthesis of $\text{KTiNbO}_{5-x}\text{N}_x$ and $\text{HTiNbO}_{5-x}\text{N}_x$

The resulting layered KTiNbO_5 sample was subjected to calcination under ammonia gas flow at 500°C , 600°C and 700°C at $4^\circ\text{C}/\text{min}$ ramp respectively for 2 h. The horizontal tube furnace with tight end-caps was used for nitriding treatment of the samples. Initially Argon gas flows for 15 min to ensure all the air is removed from quartz tube, then ammonia gas flow started subsequently raising the temperature to desired value. The product was cooled down to room temperature and Argon gas flows again to remove ammonia remaining in the tube. The HTiNbO_5 sample were treated at 250°C , 350°C and 450°C in ammonia gas for 30 min, respectively. In this paper, $\text{KTiNbO}_{5-x}\text{N}_x$ (500°C , 2 h) stands for KTiNbO_5 sample and nitriding treatment at 500°C for 2 h. Other samples are represented as the same.

Characterization

Crystal phase analysis were made by X-ray diffraction (XRD) using a Miniflex 600 X-ray diffractometer with monochromatic $\text{Cu K}\alpha$ radiation ($\lambda=0.1542$ nm, accelerating voltage 40 kV, applied current 15 mA) at scanning speed of $1^\circ/\text{min}$. Morphological analysis and compositions were confirmed using scanning electron microscopy (SEM) instrument (JSM-7800F, Japan). Hitachi U-3900 spectrophotometer was used to get UV-Vis Diffuse Reflectance Spectra in the range of 200–850 nm, using BaSO_4 standard as the reference. XPS measurements were carried out on an X-ray photoelectron spectrometer (ESCALAB250Xi) using Al $\text{K}\alpha$ (1486.6 eV) X-rays as the excitation source. C 1s (284.5 eV) was chosen as the reference. Horiba FL3-111 is used to analyze photoluminescence spectra of all the samples.

Photocatalytic experimental procedure: degradation of Rhodamine B (RhB)

For the photocatalytic degradation reaction, an open jacketed glass vessel has been used keeping the temperature constant at atmospheric conditions. 15 ppm solution (200 ml) of RhB containing 120 mg of photocatalyst was used as initial conditions. Before light irradiation, the suspension was equilibrated for 60 min in dark after which irradiated under continuous stirring using a visible light (300 W Microsolar 300 UV-Xe lamp with a UV-cutoff filter (420 nm) and was positioned 15 cm far from the reactor (removing the effect of light on photocatalysis). Sampling was performed every 10 min for evaluation of reaction kinetics with a UV-Vis absorption (Hitachi U-3900 spectrophotometer) at the characteristic absorption peak of 554 nm (λ_{RhB}) for RhB.

Results and Discussion

Structural and morphological analysis

Titanate samples (KTiNbO_5 and HTiNbO_5) usually have a layered structure. **Figure 1** shows the XRD patterns of as-prepared

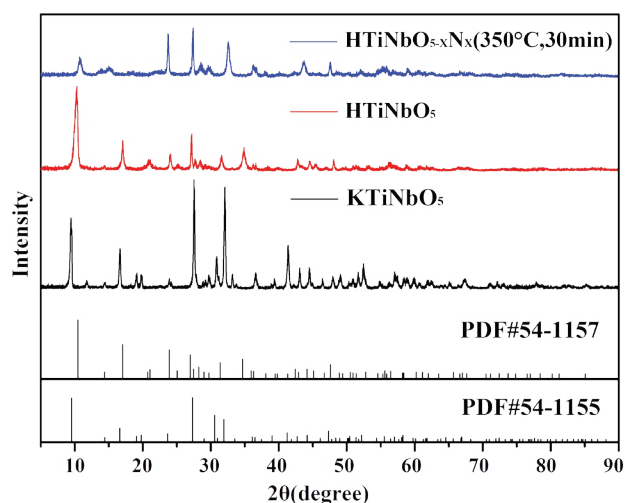


Figure 1 XRD patterns of KTiNbO_5 , HTiNbO_5 and $\text{HTiNbO}_{5-x}\text{N}_x$ after nitrogen doping at 350°C samples.

KTiNbO_5 samples before and after treatment. It can be seen that all patterns of KTiNbO_5 matches well with the standard data (JCPDS No. 54-1155) and exhibited good crystallinity [10]. Supplementary **Figure S1(a)** represents a lattice structure of KTiNbO_5 , as it is composed of corrugated sheets structure oxides with MO_6 octahedra ($M=\text{Ti, Nb}$). These kinds of structure have a low layer charge density and extraordinary ion exchange capacity [16]. After proton-exchange (HTiNbO_5), the sample can be well indexed according to standard data (JCPDS No. 54-1157 in **Figure 1**). Conferring to the position of the characteristic (002) surface, $2\theta=10.56^\circ$) reflection of the layered structure (Supplementary **Figure S1(b)**), the interlayer distance of HTiNbO_5 is calculated to be 8.57 \AA . Further, the diffraction peak intensity at low angle ($2\theta \approx 10.56^\circ$) was observed to decrease for $\text{HTiNbO}_{5-x}\text{N}_x$ (350°C , 30 min) sample after nitriding by ammonia gas with some obvious peak shift towards large angle. For N-doped KTiNbO_5 samples (Supplementary **Figure S2**) synthesized at 500 , 600 and 700°C , respectively, there is no significant change in peaks thus ensures that the layered structure is reserved but the intensity of the peaks was observed to reduce. It is mainly due to the defect induced by nitriding treatment. XRD patterns of N-doped HTiNbO_5 samples with different nitriding conditions are shown in Supplementary **Figure S3**. The lower nitriding temperatures have caused obvious change of peak pattern. With the increase of nitriding temperature, some peaks observed to shift for higher diffraction angles even reduced or disappeared. This is caused by the decrease of interplanar spacing and some defect that are induced by nitrogen doping. Totally, an obvious shift of peaks for N doped HTiNbO_5 sample at low nitriding temperatures can be seen clearly, but almost no change was observed for N doped KTiNbO_5 in high nitriding temperature except the intensity of peaks (Supplementary **Figures S2 and S3**).

As shown in **Figure 2a**, the layered metal oxides (KTiNbO_5) were made up of tabular particles with the size of $2-5 \mu\text{m}$. **Figure 2b** shows the topography of protonated HTiNbO_5 sample. It is observed that curing does not affect the lamellar structure of the virgin HTiNbO_5 , as plates are stacked together in ordered

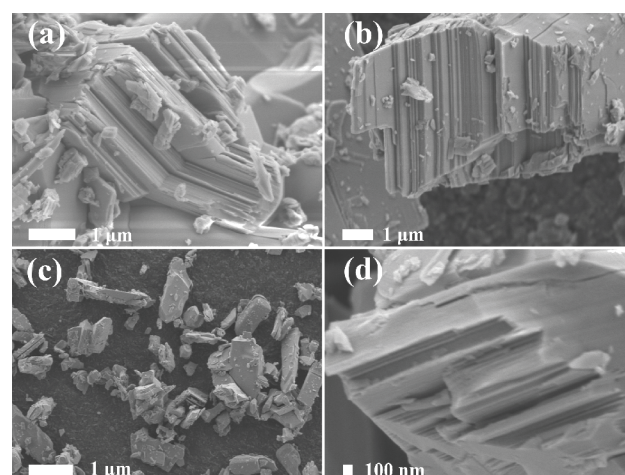


Figure 2 Typical FESEM of (a) KTiNbO_5 , (b) HTiNbO_5 , (c) and (d) of HTiNbO_5 after nitrogen doping at 350°C .

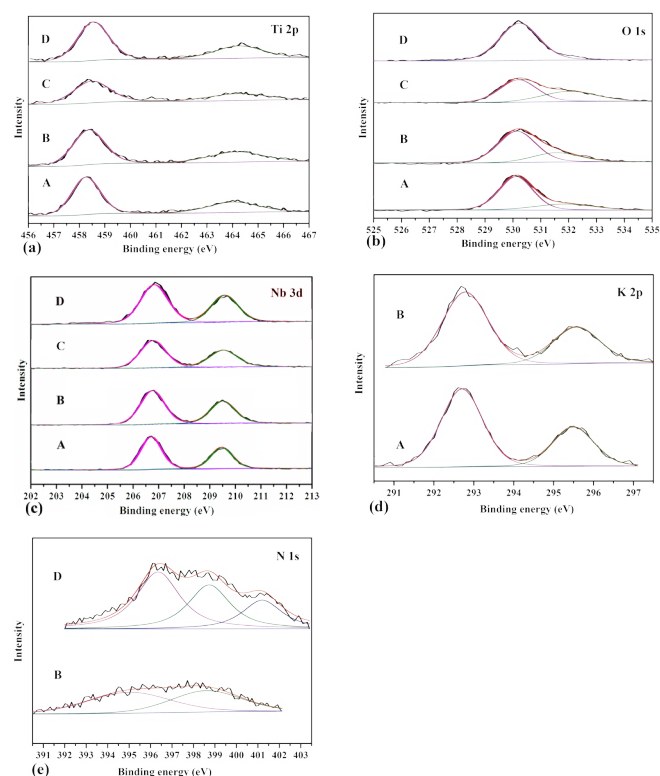


Figure 3 XPS spectra for (a) $\text{Ti}(2p)$, (b) $\text{O}(1s)$, (c) $\text{Nb}(3d)$, (d) $\text{K}(2p)$ and (e) $\text{N}(1s)$ signals of (A) KTiNbO_5 , (B) $\text{KTiNbO}_{5-x}\text{N}_x$ (500°C , 2 h), (C) HTiNbO_5 and (D) $\text{HTiNbO}_{5-x}\text{N}_x$ (350°C , 30 min).

form yielding a sheet like structure in micrometer range. After nitriding treatment at 350°C for 30 min under ammonia gas, the resulting sample showed a similar morphology to HTiNbO_5 . However, it should be noted that layered $\text{HTiNbO}_{5-x}\text{N}_x$ (350°C , 2h) (**Figures 2c and 2d**) consist of smaller particles and some lamellar character was not obvious, which could be ascribed to the nitriding conditions employed in the preparation of the products. Morphological analysis is well in accordance with structural analysis of the samples obtained from XRD.

XPS analysis and diffused reflectance spectra

In order to confirm the effect of nitrogen doping on the electronic states of the elements present, XPS binding energies have been observed for all the prepared samples. **Figure 3** represents the elemental survey spectrum of Ti 2p, O 1s, Nb 3d, K 2p and N 1s for KTiNbO_5 , $\text{KTiNbO}_{5-x}\text{N}_x$ (500°C, 2 h), HTiNbO_5 and $\text{HTiNbO}_{5-x}\text{N}_x$ (350°C, 30 min) samples. Generally, the peak at around 530 eV is assigned to the Ti-O bonds [17] and the peak around 458 eV (Ti $2P_{3/2}$ levels) corresponds to Ti^{4+} [18]. In KTiNbO_5 and $\text{KTiNbO}_{5-x}\text{N}_x$ (500°C, 2 h) samples, the binding energies of Ti $2p_{3/2}$, O 1s and Nb $3d_{5/2}$ are shifted from 458.38, 530.15 and 206.76 eV to 458.26, 530.12 and 206.71 eV, respectively. The amplified surface electron densities of Ti, O and Nb by relieving lattice O atoms with N atoms (smaller electronegativity) have caused the phenomenon. However, no binding energy shift was observed for K 2p after nitrogen doping. Compared with the peaks of HTiNbO_5 sample, the binding energy shift of Ti, O and Nb in protonated HTiNbO_5 after nitrogen doping is only 0.03-0.08 eV. This small shift of the binding energy is mainly due to that the substitutional N have declining effect on the outer electron densities of Ti, O and Nb when associated with H which has strong electronegativity. Another noteworthy characteristic is the clear increase in Ti 2p, O 1s and Nb 3d peak intensity after nitrogen doping in $\text{HTiNbO}_{5-x}\text{N}_x$ (350°C, 30 min) that can be ascribed probably to the establishment of the more Ti-N bonds [19]. Generally, the peak around 397 eV represents the existence of N-Ti-O bonds (substitution of N ion for O ion). The XPS peak at 400 eV can be allocated to interstitial N [20-21]. Therefore, peaks at the binding energies of 395.07, 398.68 eV and 396.35, 398.73 eV for $\text{KTiNbO}_{5-x}\text{N}_x$ (500°C, 2 h) and $\text{HTiNbO}_{5-x}\text{N}_x$ (350°C, 30 min) samples, respectively apportioned to substitutional N legitimately. As for the state of nitrogen species at 401.2 eV in $\text{HTiNbO}_{5-x}\text{N}_x$ (350°C, 30 min), we tend to believe that it is originated from adsorbed nitrogen species or interstitial N. The total amount of N in $\text{HTiNbO}_{5-x}\text{N}_x$ (350°C, 30 min) sample is 6.15 atom %, where substitution N occupies the major percentage of total. Although the nitriding temperature is high (500°C), the amount of doped N for $\text{KTiNbO}_{5-x}\text{N}_x$ (500°C, 2 h) is only 1.87 atom %. As we have explored previously that, the substitutional N plays a key role in mixing N 2p with O 2p states and the band gap narrowing.

The above results are well in accordance with UV-Vis DRS of the samples. Before proton-exchange, KTiNbO_5 samples were treated by ammonia gas at 500°C, 600°C and 700°C for 2 h, respectively. In contrast to the pristine layered KTiNbO_5 , the absorbance threshold of $\text{KTiNbO}_{5-x}\text{N}_x$ (500°C, 600°C and 700°C, 2 h) samples have almost no change (Supplementary **Figure S4**). With an increase in the nitriding temperature, higher absorption intensity was perceived which is mainly due to the oxygen vacancies produced for maintaining the electroneutrality [22]. As shown in Supplementary **Figure S5**, the UV-Vis DRS for both KTiNbO_5 and HTiNbO_5 are almost same indicating that proton-exchange have no impact on the absorbance property of the materials. But in contrast to the primitive layered HTiNbO_5 , the absorbance thresholds of $\text{HTiNbO}_{5-x}\text{N}_x$ (250°C, 350°C and 450°C, 30 min) samples displayed an extraordinary band-to-band red shift from 380 nm to 420, 460 and 480 nm, respectively (**Figure 4**).

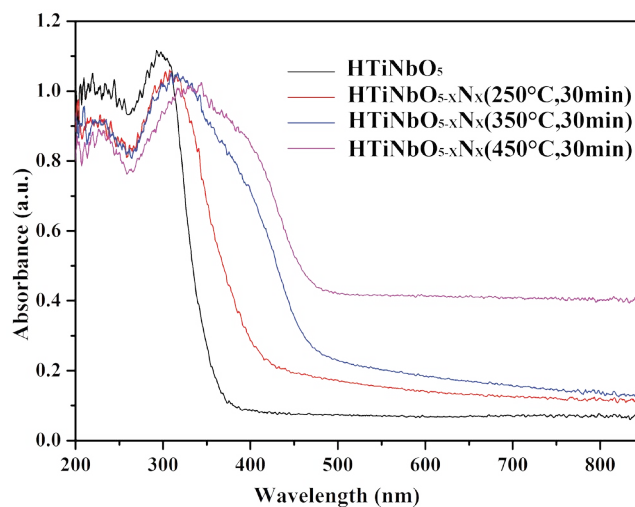


Figure 4 UV-Vis DRS of HTiNbO_5 and $\text{HTiNbO}_{5-x}\text{N}_x$ samples.

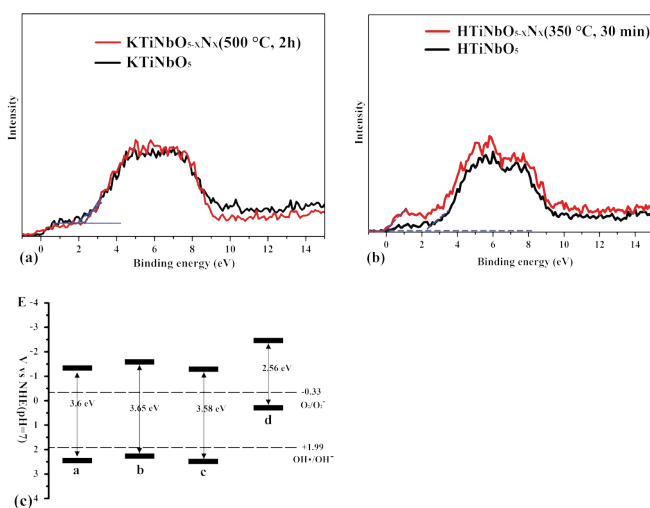


Figure 5 XPS valence band spectra of (a) KTiNbO_5 and $\text{KTiNbO}_{5-x}\text{N}_x$ (500°C, 2 h), (b) HTiNbO_5 and $\text{HTiNbO}_{5-x}\text{N}_x$ (350°C, 30 min) samples, (c) Band alignments of samples KTiNbO_5 -a, $\text{KTiNbO}_{5-x}\text{N}_x$ (500°C, 2 h)-b, HTiNbO_5 -c, $\text{HTiNbO}_{5-x}\text{N}_x$ (350°C, 30 min)-d.

In addition, the absorption intensity increases with the increase in nitriding temperature. This behavior is much diverse from the small absorption edge shift in $\text{KTiNbO}_{5-x}\text{N}_x$ samples, as shown in Supplementary **Figure S4**. It is important to note that the band-to-band absorption characteristic of the samples is not relevant to the temperature of nitriding treatment and the layered structure. As shown in Supplementary **Figure S1**, both KTiNbO_5 and HTiNbO_5 possess similar crystal structure (orthorhombic), belongs to space group $pnma$ but the bond energy of K-O is stronger than hydrogen, therefore at the same nitriding treatment temperature, KTiNbO_5 sample is hard for N doping.

As we known, the redox power of carriers plays a key role in determining the photocatalytic ability of samples, the energy levels of Valence Band Maximum (VBM) and conduction band minimum (CBM) were necessary to be confirmed. The XPS

valence band spectra of KTiNbO_5 and HTiNbO_5 were measured (Figures 5a and 5b). And it can be seen clearly the different effect of nitrogen doping on the CBM and VBM between KTiNbO_5 and HTiNbO_5 . Compared with the HTiNbO_5 , an obviously upward shift of VBM of $\text{HTiNbO}_{5-x}\text{N}_x$ (350°C, 30 min). But the upward shift was not obvious for $\text{KTiNbO}_{5-x}\text{N}_x$ (500°C, 2 h). After nitrogen doping, the valence band maximum of KTiNbO_5 and HTiNbO_5 samples are shifted from 2.2 and 2 eV to 2.26 and 0 eV, respectively. As reported by Hou et al. [15], when test in the condition of normal hydrogen electrode (NHE) at pH 7, VBM of HTiNbO_5 located at +2.41 eV. In addition, for $\bullet\text{OH}/\text{OH}^-$ and $\text{O}_2/\text{O}_2^{\bullet-}$, the redox potentials maintained at +1.99 and -0.33 eV [23,24]. Compared with the VBM value of HTiNbO_5 (+2.41 eV), the electronic potentials for the other samples can be determined (Figure 5c). The potential of holes in $\text{HTiNbO}_{5-x}\text{N}_x$ (350°C, 30 min) are higher than the potential of $\bullet\text{OH}/\text{OH}^-$ that caused by nitrogen doped HTiNbO_5 . So it cannot oxidize OH^- into $\bullet\text{OH}$. And for KTiNbO_5 , $\text{KTiNbO}_{5-x}\text{N}_x$ (500°C, 2 h) and HTiNbO_5 samples, the oxidation ability is not strong enough. Moreover, the level of CBM of all samples is negative enough to allow the single-electron reduction reaction of oxygen ($\text{O}_2 + e^- \rightarrow \text{O}_2^{\bullet-}(\text{aq})$, -0.33 V vs. NHE). But the bandgap of KTiNbO_5 , $\text{KTiNbO}_{5-x}\text{N}_x$ (500°C, 2 h) and HTiNbO_5 are too wide to precede the photocatalysis reaction. Thus, with proper bandgap and more negative level of CBM than the redox potentials of single-electron reduction of oxygen, $\text{HTiNbO}_{5-x}\text{N}_x$ (350°C, 30 min) is more suitable for using in photocatalytic reaction than other three.

Photocatalytic analysis and photoluminescence spectra

Figure 6a shows the percentage degradation of RhB under visible light irradiation in the presence of prepared titanate samples. The photocatalyst and dye was equilibrated for 60 min prior to light irradiation. No change was observed in maximum absorbance (554 nm) in the absence of light. The percentage degradation rate of RhB was calculated using $(\text{PDE} = (C_0 - C_t)/C_0)$. $\text{KTiNbO}_{5-x}\text{N}_x$ (500°C, 2 h) sample shows no photocatalytic activity as can be seen in the Figure 6a. Owing to large band gap (3.65 eV), $\text{KTiNbO}_{5-x}\text{N}_x$ (500°C, 2 h) cannot be activated by visible light. The small degradation can be accorded to either dye adsorbed on the surface of the catalyst or self-sensitization. After proton-exchange and nitrating treatment, the photocatalytic degradation efficiency of RhB for $\text{HTiNbO}_{5-x}\text{N}_x$ (350°C, 30 min) was found to be 73 %. The enhanced visible light photocatalytic response of $\text{HTiNbO}_{5-x}\text{N}_x$ (350°C, 30 min) can be clearly attributed to its certainly N doping ability, band to band visible light excitation, more $\bullet\text{O}_2^-$ radical and proper amount of oxygen vacancies. Figure 6b shows representative timely reduction in the maximum absorbance of RhB ($\lambda_{\text{max}} = 554$ nm) under visible light irradiation for the $\text{HTiNbO}_{5-x}\text{N}_x$ (350°C, 30 min) sample. The characteristic absorption of RhB decreases obviously as the irradiation time increases, the hypsochromic shift of the absorption maximum was obvious, indicating that N-deethylation and a dominant cleavage of the whole conjugated chromophore structure produced at the same time. Although $\text{HTiNbO}_{5-x}\text{N}_x$ (450°C, 30 min) sample absorb more visible light, but the photocatalytic performance of this sample is much lower than $\text{HTiNbO}_{5-x}\text{N}_x$ (350°C, 30 min), this can be ascribed possibly to the higher density of oxygen vacancies which served as

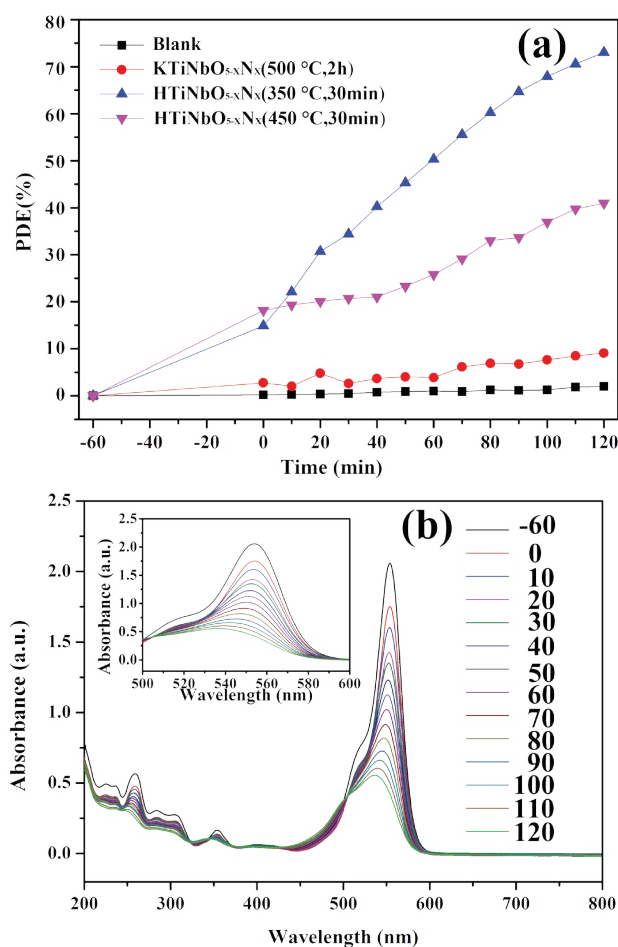


Figure 6 (a) Time-dependent photocatalytic degradation of RhB solution upon exposure to visible light using the obtained KTiNbO_5 , HTiNbO_5 , $\text{HTiNbO}_{5-x}\text{N}_x$ (350°C, 30 min) and $\text{HTiNbO}_{5-x}\text{N}_x$ (450°C, 30 min) samples, Representative variations of the characteristic absorption of RhB (b) under visible light irradiation by using $\text{HTiNbO}_{5-x}\text{N}_x$ (350°C, 30 min) (-60 to 0 as absorb time, 0-120 as photocatalysis time).

recombination centers leading to a decrease in the photocatalytic activity. Photoluminescence (PL) spectra of undoped and nitrogen doped KTiNbO_5 and HTiNbO_5 samples with excitations at 300 nm were recorded and presented in Figure 7. The broad emission in the spectral range from 320 to 450 nm was observed, which is known as charge transfer emission band. While we observed low energy band range from 450 to 500 nm, these bands are attributed to oxygen vacancies or defects sites. Therefore, emissions likely originated from surface defects, such as ionizable oxygen vacancies and the recombination of self-trapped excitons (STEs) of metal oxide semiconductors which are localized within metal oxide lattice sites [25-26].

Moreover the PL intensities resulting from efficient charge separation was altered for KTiNbO_5 and HTiNbO_5 doped with nonmetal. The lower PL intensities were also reported to exhibit higher photocatalytic activity. From our observation PL intensity was decreased for N doped KTiNbO_5 and HTiNbO_5 samples than pristine KTiNbO_5 and HTiNbO_5 , therefore we can consider that,

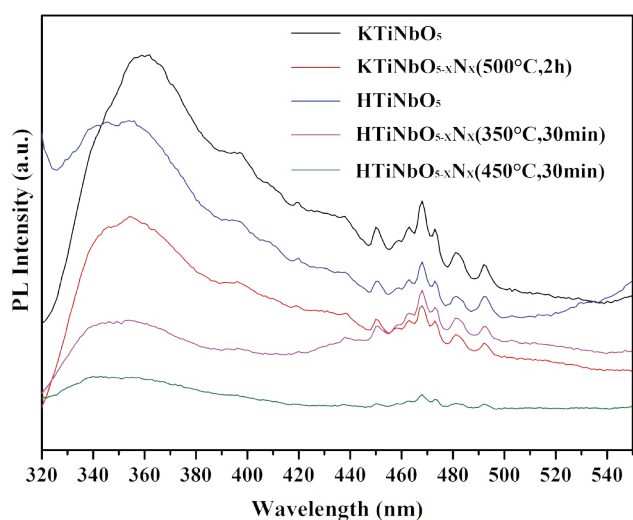


Figure 7 Photoluminescence spectra of KTiNbO_5 , $\text{KTiNbO}_{5-x}\text{N}_x$ (500°C , 2 h), HTiNbO_5 , $\text{HTiNbO}_{5-x}\text{N}_x$ (350°C , 30 min) and $\text{HTiNbO}_{5-x}\text{N}_x$ (450°C , 30 min) samples at room temperature.

the N doped KTiNbO_5 and HTiNbO_5 samples presumes good photocatalytic activity than pristine KTiNbO_5 and HTiNbO_5 . Since $\text{HTiNbO}_{5-x}\text{N}_x$ (450°C , 30 min) sample had low PL intensity but controversial photocatalytic behavior was observed. It indicates that large number of oxygen vacancies or defects couldn't influence the photocatalytic activity. $\text{HTiNbO}_{5-x}\text{N}_x$ (350°C , 30 min) sample had small PL intensity, it means reasonable oxygen vacancies or surface defects and showed efficient photocatalytic activity among all other samples.

Conclusion

Ion-exchange and nitrogen doping was realized in layered

titanates (KTiNbO_5), which leads to extraordinary band-to-band visible light excitation and high visible light photocatalytic activity. This efficient doping strategy distinctly decreases the bandgap of HTiNbO_5 from 3.58 to 2.56 eV. The nitrogen doped form and band alignments as evidenced by photoelectron spectroscopy, confirmed to be responsible for the upshift of valence band maximum of $\text{HTiNbO}_{5-x}\text{N}_x$ (350°C , 30 min). The much stronger reductive potential of generated electron in $\text{HTiNbO}_{5-x}\text{N}_x$ (350°C , 30 min) upon visible light excitation around 2.08 eV than $\text{O}_2/\text{O}_2^{\bullet-}$, narrow bandgap and oxygen vacancies induced by nitrogen doping contributes to its high visible-light photocatalytic activity in decomposing organic molecules. At low temperature nitrating treatment by ammonia gas, the N doped content in HTiNbO_5 sample reach to 6.15%. It is mainly due to the weak binding energy of hydrogen bond. This finding is of significant importance not only because a highly active visible-light photocatalyst is developed using a simple doping route but it advances the understanding of the more effective nitrogen doping in layered structure photocatalysts after ion-exchange by H^+ ions.

Acknowledgements

This work is supported by National Natural Science Foundation of China through grant 21471147 and Liaoning Provincial Natural Science Foundation through grant 2014020087. Yang M, would like to thank for the National "Thousand Youth Talents" program of China.

Conflict of Interest

This manuscript has been read and approved by all the authors. The criteria for authorship have been met. The authors also do not have any financial interest or any other conflict of interests. Lastly, this paper or any part of this study has not been submitted to any publication yet.

References

- 1 Choi W, Yeo J, Ryu J, Tachikawa T, Majima T (2010) Photocatalytic Oxidation Mechanism of As(III) on TiO₂: Unique Role of As(III) as a Charge Recombinant Species. *Environ Sci Technol* 44: 9099-9104.
- 2 Chen X, Mao SS (2007) Titanium dioxide nanomaterials: Synthesis, properties, modifications, and applications. *Chem Rev* 107: 2891-2959.
- 3 Quan F, Hu Y, Zhang X, Wei CH (2014) Simple preparation of Mn-N-codoped TiO₂ photocatalyst and the enhanced photocatalytic activity under visible light irradiation. *Appl Surf Sci* 320: 120-127.
- 4 Borgarello E, Kiwi J, Gratzel M, Pelizzetti E, Visca M (1982) Visible-Light Induced Water Cleavage in Colloidal Solutions of Chromium-Doped Titanium-Dioxide Particles. *J Am Chem Soc* 104: 2996-3002.
- 5 Choi WY, Termin A, Hoffmann MR (1994) The Role of Metal-Ion Dopants in Quantum-Sized TiO₂-Correlation between Photoreactivity and Charge-Carrier Recombination Dynamics. *J Phys Chem* 98: 13669-13679.
- 6 Izumi Y, Itoi T, Peng S, Oka K, Shibata Y (2009) Site Structure and Photocatalytic Role of Sulfur or Nitrogen-Doped Titanium Oxide with Uniform Mesopores under Visible Light. *J Phys Chem C* 113: 12926-12926.
- 7 Yang G, Hou WH, Feng XM, Jiang XF, Guo J (2007) Density functional theoretical studies on polyaniline/HNb(3)O(8) layered nanocomposites. *Adv Funct Mater* 17: 3521-3529.
- 8 Tagusagawa C, Takagaki A, Hayashi S, Domen K (2008) Efficient utilization of nanospace of layered transition metal oxide HNbMoO(6) as a strong, water-tolerant solid acid catalyst. *J Am Chem Soc* 130: 7230.
- 9 Liu G, Wang LZ, Sun CH, Yan XX, Wang XW, et al. (2009) Band-to-Band Visible-Light Photon Excitation and Photoactivity Induced by Homogeneous Nitrogen Doping in Layered Titanates. *Chem Mater* 21: 1266-1274.
- 10 Im M, Kweon SH, Kim JS, Nahm S, Choi JW, et al. (2014) Microstructural variation and dielectric properties of KTiNbO₅ and K₃Ti₅NbO₁₄ ceramics. *Ceram Int* 40: 5861-5867.
- 11 Zhai Z, Huang YC, Xu L, Yang XY, Hu CH, et al. (2011) Thermostable nitrogen-doped HTiNbO₅ nanosheets with a high visible-light photocatalytic activity. *Nano Res* 4: 635-647.
- 12 Zhai Z, Hu CH, Yang XY, Zhang LH, Liu C, et al. (2012) Nitrogen-doped mesoporous nanohybrids of TiO₂ nanoparticles and HTiNbO₅ nanosheets with a high visible-light photocatalytic activity and a good biocompatibility. *J Mater Chem* 22: 19122-19131.
- 13 Serpone N (2006) Is the band gap of pristine TiO₂ narrowed by anion- and cation-doping of titanium dioxide in second-generation photocatalysts? *J Phys Chem B* 110: 24287-24293.
- 14 Qiu YF, Wang L, Leung CF, Liu GJ, Yang SH, et al. (2011) Preparation of nitrogen doped K₂Nb₄O₁₁ with high photocatalytic activity for degradation of organic pollutants. *Appl Catal a-Gen* 402: 23-30.
- 15 Hou JG, Cao R, Wang Z, Jiao SQ, Zhu HM (2012) Hierarchical nitrogen doped bismuth niobate architectures: Controllable synthesis and excellent photocatalytic activity. *J Hazard Mater* 217: 177-186.
- 16 Sklute EC, Eguchi M, Henderson CN, Angelone MS, Yennawar HP, et al. (2011) Orientation of Diamagnetic Layered Transition Metal Oxide Particles in 1-Tesla Magnetic Fields. *J Am Chem Soc* 133: 1824-1831.
- 17 Rengifo-Herrera JA, Mielczarski E, Mielczarski J, Castillo NC, Kiwi J, et al. (2008) Escherichia coli inactivation by N, S co-doped commercial TiO₂ powders under UV and visible light. *Appl Catal B-Environ* 84: 448-456.
- 18 Breault TM, Bartlett BM (2012) Lowering the Band Gap of Anatase-Structured TiO₂ by Coalloying with Nb and N: Electronic Structure and Photocatalytic Degradation of Methylene Blue Dye. *J Phys Chem C* 116: 5986-5994.
- 19 Batzill M, Morales EH, Diebold U (2007) Surface studies of nitrogen implanted TiO₂. *Chem Phys* 339: 36-43.
- 20 Wang J, Tafen DN, Lewis JP, Hong ZL, Manivannan A, et al. (2009) Origin of Photocatalytic Activity of Nitrogen-Doped TiO₂ Nanobelts. *J Am Chem Soc* 131: 12290-12297.
- 21 Chong MN, Jin B, Chow CWK, Saint C (2010) Recent developments in photocatalytic water treatment technology: A review. *Water Res* 44: 2997-3027.
- 22 Daghrih R, Drogui P, Robert D (2013) Modified TiO₂ For Environmental Photocatalytic Applications: A Review. *Ind Eng Chem Res* 52: 3581-3599.
- 23 Liu C, Han RR, Ji HM, Sun T, Zhao J, et al. (2016) S-doped mesoporous nanocomposite of HTiNbO₅ nanosheets and TiO₂ nanoparticles with enhanced visible light photocatalytic activity. *PCCP* 18: 801-810.
- 24 Mrowetz M, Balcerski W, Colussi AJ, Hoffmann MR (2004) Oxidative power of nitrogen-doped TiO₂ photocatalysts under visible illumination. *J Phys Chem B* 108: 17269-17273.
- 25 Watanabe M, Hayashi T (2005) Time-resolved study of self-trapped exciton luminescence in anatase TiO₂ under two-photon excitation. *J Lumin* 112: 88-91.
- 26 Ganeshraja AS, Thirumurugan S, Rajkumar K, Zhu K, Wang Y, et al. (2016) Effects of structural, optical and ferromagnetic states on the photocatalytic activities of Sn-TiO₂ nanocrystals. *RSC Adv* 6: 409-421.